MANY-BODY APPROACH TO ALPHA AND CLUSTER RADIOACTIVITY

R. Blendowske, T. Fliessbach, H. Walliser
Universität-GH-Siegen, Fachbereich Physik
59 Siegen, Germany

TABLE OF CONTENTS

Published in *Nuclear Decay Modes* ed. by D. N. Poenaru, IOP Publishing, Bristol 1996

I. DECAY CONSTANT

A. Introduction

Cluster radioactivity is the spontaneous decay of nuclei by the emission of clusters like for example α-particles, C-, Ne-, Mg- or Si-nuclei. The spontaneous emission of clusters heavier than α-particles is called exotic decay.

The traditional α-decay theory can be extended to the exotic decays.[1,2,3] After a short presentation of the underlying physical model we define and evaluate Gamow's decay constant and the spectroscopic factor (this section). In Section II the model expression for the decay constant is applied to a representative sample of exotic decays. The results are further discussed in Section III. This handbook article is restricted to the basic formulae. It contains, however, all information necessary for the easy application to other decays.

We consider the decay of a nucleus with $(A+a)$ nucleons and $(Z+z)$ protons

$$ {}^{A+a}(Z+z) \longrightarrow {}^{A}Z + {}^{a}z. \tag{1} $$

In the energy regime of interest, the nuclei are well described as many-body systems of nucleons. The bound many-body wave functions of the parent and daughter nucleus and of the emitted cluster are denoted by

$$ \phi_{A+a}\,,\ \phi_A\,,\ \phi_a. \tag{2} $$

The open exit channel in (1) is made up by ϕ_A and ϕ_a. The decay is due to the coupling of the initial state ϕ_{A+a} to this exit channel. The process is treated in the following model: With a certain probability S the parent nucleus wave function ϕ_{A+a} lies in the open channel space $\phi_A \otimes \phi_a$. Only this part of the wave function contributes to the decay (1). Within the space $\phi_A \otimes \phi_a$ the problem reduces to a one-body problem, that means to the determination of the relative motion between the daughter nucleus and the emitted cluster. The relative motion amplitude penetrates through the Coulomb barrier and determines the decay constant.

This model leads to a decay constant of the form

$$ \lambda = \lambda_{\mathrm{G}}\, S, \tag{3} $$

where the spectroscopic factor S is the probability of finding the structure $\phi_A \otimes \phi_a$ in the parent nucleus, and λ_{G} is the Gamow decay constant of the reduced one-body problem. The information about the many-body structure is contained in the spectroscopic factor. The half-life is given by $\tau = \ln 2/\lambda$.

B. Gamow Decay Constant

In this subsection we evaluate the one-body decay constant λ_{G}. Gamow's one-body model explains the Geiger Nuttall law, i.e. the strong variation of the half-lives with the decay energy. In some form it is contained in every approach to α- and exotic decays, including macroscopic fission models.[4]

The decay constant $\lambda_{\rm G}$ can be evaluated with sufficient accuracy by using the semiclassical WKB approximation

$$\lambda_{\rm G} \approx \frac{v}{2R_{\rm i}} \, \exp\left(-2 \int_{R_{\rm i}}^{R_{\rm o}} dR \, \sqrt{\frac{2\mu}{\hbar^2} \left[V(R) - E_{aA} \right]} \right). \tag{4}$$

This decay constant is the product of the knocking frequency $\nu = v/2R_{\rm i}$ and the barrier penetrability. The inner and outer turning point, $R_{\rm i}$ and $R_{\rm o}$, are determined by the condition that the potential $V(R)$ equals the tunneling energy E_{aA}. The reduced mass of the emitted fragments is denoted by μ. For the fragment interaction we use the semiempirical heavy ion potential

$$\begin{aligned} V(R) &= -\frac{50\,\text{MeV}}{\text{fm}} \, \frac{R_a R_A}{R_a + R_A} \, \exp\left(\frac{R_a + R_A - R}{d} \right) + \frac{zZe^2}{R} \\ d &= 0.63 \text{ fm}, \qquad R_n = \left(1.233\, n^{1/3} - 0.978\, n^{-1/3} \right) \text{fm}, \quad n = a \text{ or } A \end{aligned} \tag{5}$$

fitted to elastic scattering data.[5] This potential can be applied to α-decay and to exotic decays as well. At the inner turning point $R_{\rm i}$ the two fragments are just beginning to feel the nuclear interaction. In (4) the potential $V(R)$ is used for radii $R \geq R_{\rm i}$ only, i.e. for radii where it is reasonably well determined from scattering experiments.

If the angular momentum of the emitted cluster is known a centrifugal term might be added to (5). However, such a term – as well as the deviation of the Coulomb potential from zZe^2/R – has only a negligible effect on the barrier penetrability; therefore these contributions are omitted.

The tunneling energy E_{aA} is given by

$$E_{aA} = \left(M_{A+a} - M_A - M_a \right) c^2 - E^{\rm ex}. \tag{6}$$

The M_i are the rest masses of the bare nuclei stripped from electrons. Since usually the masses of neutral atoms are listed[6] the extracted Q-values have to be corrected for the small electronic binding energies.[7] This small correction has some effect on $\lambda_{\rm G}$ because the penetrability depends sensitively on the tunneling energy. The tunneling energy (6) is diminuished by a possible excitation energy $E^{\rm ex}$ of the fragments.

In the interior ($R \leq R_{\rm i}$) the kinetic energy $\mu\, v^2/2$ equals approximately the potential depth. A realistic potential depth is of the order $a \cdot 25\,\text{MeV}$ corresponding to a 100 MeV deep α-nucleus-potential. The knocking frequency becomes then

$$\nu = \frac{v}{2R_{\rm i}} = \sqrt{\frac{a \cdot 25\ \text{MeV}}{2\mu {R_{\rm i}}^2}}. \tag{7}$$

The frequency ν is nearly constant for all decay modes since the reduced mass μ scales roughly with a.

The results of the WKB approximation (4)–(7) have been compared to exact solutions of the Schrödinger equation of the reduced one-body problem.[3] It has been found that in the considered range of fragments and decay energies the error is less than a factor of two. This is comparable to the uncertainty due to the specific choice of the potential $V(R)$.

C. Spectroscopic Factor

In this subsection we define the spectroscopic factor S on the basis of the many-body states (2). The structure of the resulting expression and explicit numerical evaluations lead to a semiempirical approximate formula for S. This formula allows a unified (valid for different cluster sizes) and simple description of favoured decays.

The open channel state describes the relative motion of the clusters ϕ_a and ϕ_A. It is therefore a superposition of the basis states

$$\langle \mathbf{r}_1, ..., \mathbf{r}_{A+a-1} \,|\, \mathbf{R} \,\rangle = \mathcal{A}\left(\delta(\mathbf{R} - \mathbf{r}_{aA})\, \phi_a\, \phi_A\right) \tag{8}$$

with different values of $\mathbf{R}$. In coordinate space the states $|\mathbf{R}\rangle$ depend on $(A + a - 1)$ coordinates which are equivalent to the $(A - 1)$ internal coordinates of the daughter nucleus ϕ_A, the $(a - 1)$ internal coordinates of the emitted fragment and the relative motion coordinate $\mathbf{r}_{aA}$. Due to the antisymmetrization $\mathcal{A}$ the states $|\mathbf{R}\rangle$ are not normalized

$$\langle\, \mathbf{R} \,|\, \mathbf{R}' \,\rangle = \left(1 - \widehat{K}\right)_{\mathbf{R},\mathbf{R}'} = \delta(\mathbf{R} - \mathbf{R}') - \, K(\mathbf{R},\, \mathbf{R}') \; . \tag{9}$$

We define the projection operator $\widehat{P}$ onto the open channel space $\{|\, \mathbf{R} \,\rangle\}$

$$\widehat{P} = \int d^3R \int d^3R' \;\; |\, \mathbf{R} \,\rangle \;\left(\frac{1}{1 - \widehat{K}}\right)_{\mathbf{R},\mathbf{R}'} \langle\, \mathbf{R}' \,| \; . \tag{10}$$

The inverse of the norm operator $1 - \widehat{K}$ guarantees that $\widehat{P}^{\,2} = \widehat{P}$; this condition is a necessity for a projection operator. The *spectroscopic factor*

$$S \;=\; \left\langle \phi_{A+a} \,\middle|\, \widehat{P} \,\middle|\, \phi_{A+a} \right\rangle \tag{11}$$

equals the percentage to which the state ϕ_{A+a} lies in the space $\phi_A \otimes \phi_a$ spanned by (8). In other words, it is the quantum mechanical probability of finding the open channel structure preformed in the parent nucleus. Therefore S may also be called *preformation probability*.

Cluster spectroscopic factors found in the literature before 1975 neglect the effect of the norm operator; they are indeed obtained from (11) and (10) with $\widehat{K} = 0$. The operator (10) with $\widehat{K} \;=\; 0$ is, however, no longer a projection operator, and consequently (11) is not a properly defined quantum mechanical probability. The neglect of the proper normalization results in spectroscopic factors which are too small by many orders of magnitude for heavy fragments.

After a suitable choice for the many-body wave functions (2) the spectroscopic factor (11) is fixed and may be calculated. Such microscopic calculations have been presented for α-decay[8,9] and for ^{14}C-decay.[1] The many-body states employed are those of the spherical nuclear shell model including configuration mixing. These calculations lead to the following orders of magnitude for the spectroscopic factor:

$$S \sim \begin{cases} 10^{-2} & ^{212}\mathrm{Po} \rightarrow \alpha + ^{208}\mathrm{Pb} \\ 10^{-8} & ^{222}\mathrm{Ra} \rightarrow ^{12}\mathrm{C} + ^{210}\mathrm{Pb} \\ 10^{-10} & ^{224}\mathrm{Ra} \rightarrow ^{14}\mathrm{C} + ^{210}\mathrm{Pb} \\ 10^{-11} & ^{226}\mathrm{Th} \rightarrow ^{16}\mathrm{O} + ^{210}\mathrm{Pb} \end{cases} \tag{12}$$

The calculated numbers for S and λ_{G} of (4) yield decay constants $\lambda = \lambda_{\mathrm{G}}\, S$ which are of the right absolute size.

The performance of microscopic calculations is rather tedious, in particular because of the appearance of the norm operator $1 - \widehat{K}$ in (10). Therefore, we introduce a bulk spectroscopic factor which is simple to comprehend, easy to handle, and which covers the whole variety of favoured decays.

The spectroscopic factor (11) can be related to the squared product of the overlaps between the single particle states in ϕ_a and the upper ones in ϕ_{A+a} forming the fragment.[3] The product contains effectively $a - 1$ single particle overlaps because ϕ_a depends on $a - 1$ internal coordinates. This structure implies that many single particle states contribute to S, and that S will roughly scale with the $(a-1)$-st power of the square of a single particle overlap. The first point suggests to use a bulk formula. The second point indicates that, compared to α-spectroscopic factors S_α, the spectroscopic factors for heavier fragments should scale like

$$S_{\mathrm{bulk}} = S_\alpha^{(a-1)/3} \qquad \text{(bulk spectroscopic factor).} \tag{13}$$

The numerical expense of microscopic calculations, the uncertainties originating from the choice of the nuclear many-body wave functions, and the relatively large number of contributing single particle functions justify the use of the *bulk spectroscopic factor* for practical purposes. This will be done in the following.

The bulk spectroscopic factor will not be applicable to cases governed by specific structure effects. By specific structure effects we mean for example that the symmetry of the wave functions forbids the considered decay. For many-body states, such decays are normally not exactly forbidden but they are *hindered* or *unfavoured*; an example will be discussed in section III.A. For these unfavoured decays, eq. (3) together with the original spectroscopic factor (11) has to be used. The bulk expression (13) is adequate for the so-called favoured decays only.

II. RESULTS

Eq. (3) with (4) and (13) yields the final expression for the decay constant

$$\lambda_{\mathrm{theor}} = \lambda_{\mathrm{G}}(E_{aA})\; S_\alpha^{(a-1)/3}\;. \tag{14}$$

The sensitive dependences on E_{aA} and on a are explicitly displayed but not the less sensitive ones on A and Z. The input of the theoretical decay constant is completely fixed by the following quantities:

- Mass and proton numbers of the fragments, A, Z, a and z.
- Asymptotic energy E_{aA} of the relative motion of the fragments.
- Semiempirical potential $V(R)$ as defined in (5).
- One parameter S_α.

The parameter S_α is determined by a fit to even favoured decays up to $a = 28$:

$$S_\alpha = 6.3 \cdot 10^{-3} \tag{15}$$

In the presented form the theoretical expression (14) contains just one adjustable parameter. Moreover, the fitted value (15) is in good agreement with theoretical and experimental α-spectroscopic factors in the Pb region.

Eq. (14) constitutes a *unified* description of cluster radioactivity, ranging from α-decay to exotic decays in a wide range. It displays the systematic dependence on the mass and proton numbers, and on the tunneling energy. Judging from the results, the decay constant λ_{theor} is applicable at least up to fragment masses $a \sim 34$.

According to the introduction of the bulk spectroscopic factor (13) the application of (14) is restricted to *favoured decays only*. For unfavoured decays (i.e. for specific structure effects) eq. (3) with (11) is the valid expression.

In previous publications we used two different parameters, S_{even} and S_{odd}, for even and odd decays, respectively.[2,3] The fit for S_{odd} contained, however, some ambiguity because the fine structure of odd decays is in most cases not resolved experimentally. The measured decay constant of an odd decay might be a mixture of favoured decays (suppressed by a lower E_{aA} and thus a smaller penetrability) and unfavoured decays. We therefore decided to apply (14) to favoured decays only.

Since the expression for the theoretical decay constant can be easily evaluated we do not present an exhaustive list of decay constants. For a convenient application of our formula we offer two possibilities:

1. On request the computer code realizing (14) is available for an IBM compatible PC-AT on a $5\frac{1}{4}''$ discette (360 kB or 1.2 MB).
2. In the Appendix the expression (14) is further simplified. The resulting formula may be evaluated in a few steps on a hand-pocket calculator.

Table 1 contains a representative sample of decays from even parent to even daughter nuclei which are always favoured. All considered decays go to the fragment ground states, i.e. $E^{\text{ex}} = 0$. For the experimental data we refer the handbook contribution by Bonetti et al.[10] and references therein. Some of these decays have been correctly predicted by our formula prior to the experiment.[2]

The last entry (^{46}Ar-decay) in Table 1 is probably outside the validity range of our model. The bulk spectroscopic factor (13) scales exponentially with the fragment number a. With increasing fragment size the decay probability will eventually become unmeasurably small. In particular, our model cannot be extended to fission processes; fission is due to a different mechanism.

Table 2 and 3 present decays of odd parent nuclei to ground-state and to excited states of the daughter nucleus. Possible excitations of the cluster require more energy than that of the daughter nucleus. The lowest excitations are, therefore, those of the daughter nucleus; only these excitations are considered. All theoretical half-lives in Table 2 and 3 are calculated with the parameter (15) fixed by a fit to known even decays. Therefore, the calculated τ_{theor} are valid predictions only if the specific decay is *favoured*. For the experimental values we refer again to Bonetti.[10]

In most cases the fine structure of the odd decay is not resolved experimentally. Then it is not known to which specific daughter nucleus state the measured half-life should be attributed to. In these cases we adopt the following procedure: We assume that the measured decay is a favoured one. The experimental half-life τ_{exp} is attached tentatively to the specific transition suggested by τ_{theor}. Accordingly we classify decays into lower states as hindered or unfavoured. The sensibility of this procedure is verified in the case of the ^{14}C-decay of ^{223}Ra with known fine structure (section III.A).

III. DISCUSSION

A. Fine Structure

The presented evaluation of (3) refers to spherical nuclei; the microscopic calculations use spherical shell model functions, and λ_{G} is evaluated with the spherical potential (5). In spite of these simplifications, the expression (14) reproduces well the gross features of the considered decays. The deformation is obviously of minor importance for the overall behaviour.

For a detailed consideration of structure effects the deformation has, however, to be taken into account. On the microscopic level this can be done by using Nilsson shell model states which are classified by the usual quantum numbers $K^{\pi}[N n_z \Lambda]$. The transitions between states with different Nilsson quantum numbers are suppressed because the overlaps contained in the spectroscopic factor (11) are zero or at least particularly small. Such decays are unfavoured.

The fine structure[11] of the ^{14}C-decay of ^{223}Ra has been discussed by Hussonnois et al..[12] Following Hussonnois et al. we discuss the fine structure of this decay (shown in Figure 1) with respect to our model. Most decays (81%) lead to the first excited state of ^{209}Pb at 0.778 MeV although the penetrability for the decay to the ground state is 32 times larger. This phenomenon is clearly connected to structure effects, that means to the spectroscopic factor. The parent nucleus ^{223}Ra may be described in the rotor model by the mixed parity doublet $3/2^{\pm}[631] \otimes [761]$. The ground and excited states of the daughter nucleus ^{209}Pb have the quantum numbers

of the odd neutron in a single particle level of the spherical shell model outside the lead core. In contrast to the ground state, the first two excited states contain substantial components $3/2^+$ [631] and $3/2^-$ [761], respectively.[12] Therefore we expect that the transitions to these excited states are favoured by the internal structure.

Using the form (3) we determine experimental spectroscopic factors from

$$S_{\rm exp} = \frac{\lambda_{\rm exp}}{\lambda_{\rm G}} \ . \tag{16}$$

Gamow's decay constant $\lambda_{\rm G}$ is calculated using the tunneling energies E_{aA} given in Table 2; the excitation energies are taken into account according to (6). The resulting experimental spectroscopic factors (given in Figure 1) reflect the discussed structure effects: The decay to the ground state is unfavoured, the decays to the first excited states are favoured. For the favoured decays our bulk spectroscopic factor $S_{\rm bulk} = (6.3 \cdot 10^{-3})^{13/3} = 2.9 \cdot 10^{-10}$ from (13) and (15) agrees well with $S_{\rm exp}$.

From the experimental spectroscopic factor we see that the transition to the ground state is hindered by a factor of 150. For a microscopic description of this decay we have, in principle, to go back to the original expression (11). Microscopic evaluations of (11) for unfavoured decays are, however, difficult. They require the knowledge of the specific nuclear structure in terms of the many-body wave functions of the parent and the daughter nucleus. In addition the quite different deformations of these nuclei complicate such calculations.

As already discussed, one could try to use a bulk formula for unfavoured decays, too, using a separate parameter $S_{\alpha,\rm unfav}$ instead of (15). However, the degree of unfavouredness (due to the specific microscopic structure effects) is likely to be quite different for various nuclei. It is therefore doubtful whether a bulk formula like (13) with an extra fit parameter $S_{\alpha,\rm unfav}$ makes sense for unfavoured decays. No such attempt is made in this paper.

An evaluation of (11) for each specific final state appears not feasible. Irrespective of this restriction our model provides a qualitative understanding of the fine structure.

B. Other Approaches

The generalization of the microscopic α-decay theory leads to a successfull and consistent model of cluster radioactivity. This does not exclude the possibility of other descriptions. The obvious alternative is the treatment of exotic decays as an extremely asymmetric cold fission.[4] All existing fission models for exotic decay are restricted to one or few macroscopic degrees of freedom; in this sense they are macroscopic models. These models might be derived microscopically by evaluating the potential landscape and the inertial parameters starting from a many-body Hamiltonian.

In fission models, the deformation energy of the fissioning nucleus is parametrized versus the distance between the fragment centers or some related quantity. For separated fragments the deformation energy becomes the Coulomb plus

the centrifugal potential. The penetration of the classically forbidden deformation barrier determines the fission probability. The tunneling is usually calculated using the semiclassical WKB approximation. This leads to a decay constant $\lambda_{\rm G}^{\rm fission}$ which is of the same form (4) as our $\lambda_{\rm G}$.

The experimental decay constants are reproduced by $\lambda = \lambda_{\rm G}^{\rm fission}$ in the fission models and by $\lambda = \lambda_{\rm G}\, S$ in our approach. The preformation probabilities are quite small numbers, $S = 10^{-10}$ ... 10^{-23} (for C- to Si-decay). In order to reproduce the data the fission models must use much larger potential barriers than the ones given by (5). Effectively, our preformation probability S is replaced by the penetration factor due to an additional barrier inside the Coulomb barrier. Poenaru et al.[4] interpret this additional penetration factor as the cluster preformation probability in the fission model.

Compared to fission models our approach has the advantage of using only the outer, rather well-known part of the nuclear potential. Besides this well-known potential part, our model contains only one parameter which determines all preformation probabilities. Moreover, this model appears to be the appropriate starting point for discussing structure effects (previous subsection).

IV. SUMMARY

The excellent agreement with experimental data strongly supports the underlying physical assumption of the presented model: The decay constant $\lambda = \lambda_{\rm G}\, S$ is given by the one-body decay constant $\lambda_{\rm G}$ times the preformation probability S. From α- to Si-decay this preformation probability varies over more than 20 orders of magnitudes. The absolute size of this factor and its variation can be understood microscopically.

The presented model provides a unified description of cluster decays covering a range of emitted fragment mass numbers from $a = 4$ to $a = 34$, with half-lives from 10^{-11}s to 10^{25}s, and with branching ratios relative to α-decay from 10^{-9} to 10^{-16}. In addition, the model provides a qualitative understanding of the fine structure effects.

The theoretical expression (14) for the decay constant may be readily applied to any wanted decay. Because of the excellent reproduction of known decay rates it is well-suited for an unambiguous prediction of yet unmeasured decay constants.

APPENDIX

In this Appendix we provide a *simple analytical formula for the decay constant*. This hand-pocket formula may be used for α-decay and all exotic decays. For this purpose the realistic potential (5) is simulated by a square well with a suitable radius $R_{\rm i}$. The nearly a-independent knocking frequency $\nu = v/(2R_{\rm i})$ is fixed to an appropriate numerical value. The resulting decay constant is then given by

$$\lambda_{\rm theor} \approx \nu\; S_\alpha^{(a-1)/3}\; \exp(-2I)\,, \qquad \nu = 3.0 \cdot 10^{21}\ {\rm s}^{-1}\,, \quad S_\alpha = 6.3 \cdot 10^{-3}\,. \quad (17)$$

The penetration integral for the pure Coulomb potential can be evaluated analytically. It yields

$$I = zZe^2 \sqrt{\frac{2\mu}{\hbar^2 E_{aA}}} \left\{ \arccos\left(\sqrt{x}\,\right) - \sqrt{x - x^2}\,\right\} \tag{18}$$

with

$$x = \frac{R_\mathrm{i}\, E_{aA}}{zZe^2}\,, \qquad R_\mathrm{i} = r_0\left(a^{1/3} + A^{1/3}\right), \qquad r_0 = 1.286\ \mathrm{fm}\,.$$

In addition one needs $\hbar^2/(2\mu\,\mathrm{fm}^2) = 20.9\,\mathrm{MeV}\,(A + a)/(aA)$ and $e^2/\mathrm{fm} = 1.44\,\mathrm{MeV}$. The number for the reduced mass takes into account the mass defect in an average way (adjusted to $a = 12$).

The input for the decay constant (17) is A, Z, a, z, and E_{aA} of (6). Up to $a = 34$ all decay constants of (14) are reproduced within a factor of 3.

REFERENCES

1 Blendowske, R., Fliessbach, T. and Walliser, H., Microscopic calculation of the ^{14}C decay of Ra nuclei, *Nucl. Phys. A*, 464, 75, 1987

2 Blendowske, R. and Walliser, H., Systematics of cluster-radioactive-decay constants as suggested by microscopic calulations, *Phys. Rev. Lett.*, 61, 1930, 1988

3 Blendowske, R., Fliessbach, T. and Walliser, H., From α-decay to exotic decays – a unified model, *Z. Phys. A – Hadrons and Nuclei*, 339, 121, 1991

4 Poenaru, D. N. and Greiner, W., Fission approach to α-decay . . . , and references therein, *in this handbook*

5 Christensen, P. R. and Winther, A., The evidence of the ion-ion potentials from heavy ion elastic scattering, *Phys. Lett. B*, 65, 19, 1976

6 Wapstra, A. H. Audi, G., The 1983 atomic mass evaluation, *Nucl. Phys. A*, 432, 1, 1985

7 Huang, K. N., Aoyagi, M., Chen, M. H., Crasemann, B., Mark, H., Neutral-atom electron binding energies from relaxed-orbital relativistic Hartree-Fock-Slater calculations, *At. Data and Nucl. Data Tables* 18, 243, 1976

8 Fliessbach, T. and Mang, H. J., On absolute values of α-decay rates, *Nucl. Phys. A*, 263, 75, 1976

9 Tonozuka, I. and Arima, A., Surface α-clustering and α-decay of ^{212}Po , *Nucl. Phys. A*, 323, 45, 1979

10 Bonetti, R., Chiesa, C., Guglielmetti, A. and Migliorino, C., Experiments on fragment radioactivities . . . , and references therein, *in this handbook*

11 Hourani, E., Hussonnois, M., Carbon decay and fine structure . . . , in this handbook

12 Hussonnois, M., Le Du, J. F., Brillard, L. and Ardisson, G., Possible cluster preformation in the ^{14}C decay of ^{223}Ra , *Phys. Rev.* C 42, R495, 1990

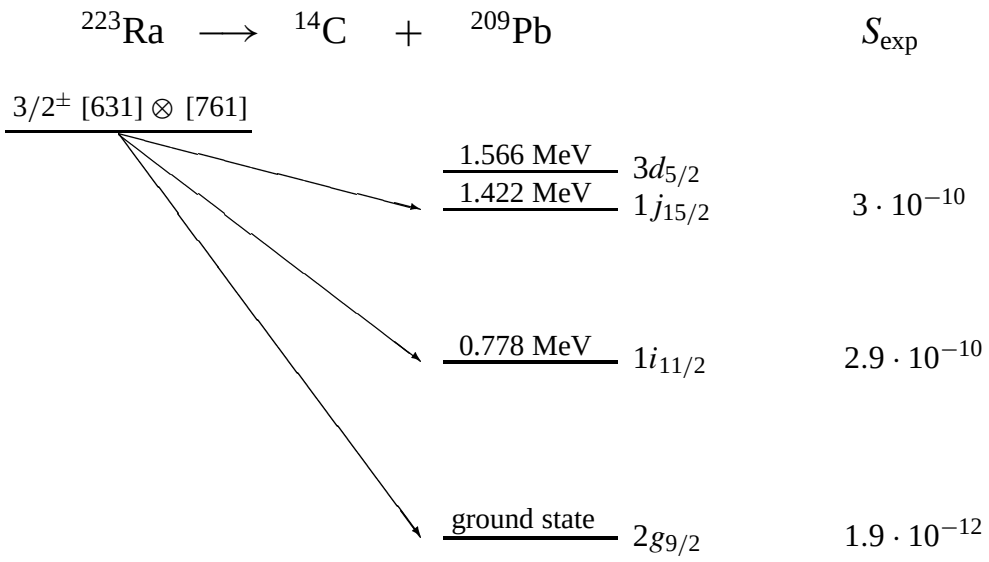

Abbildung 1: Fine structure of the ^{14}C-decay of ^{223}Ra. The decays to the first two excited states of ^{209}Pb are favoured. The experimental spectroscopic factors S_{exp} are determined from (16). For the favoured decays they are reproduced by eq. (13) with (15) yielding $S_{\text{bulk}} = 2.9 \cdot 10^{-10}$. The transition to the ground-state is hindered by a factor of 150.

$^{A+a}(Z+z)$	$\longrightarrow$	^{a}z	+	^{A}Z	E_{aA}	$\log \tau_{\text{theor}}$	$\log \tau_{\text{exp}}$
^{222}Ra	$\longrightarrow$	^{12}C	+	^{210}Pb	29.16	16.6	
	$\longrightarrow$	^{14}C	+	^{208}Pb	33.16	11.7	11.0
^{224}Ra	$\longrightarrow$	^{14}C	+	^{210}Pb	30.65	16.3	15.9
^{226}Ra	$\longrightarrow$	^{14}C	+	^{212}Pb	28.32	21.1	21.2
	$\longrightarrow$	^{20}O	+	^{206}Hg	40.97	26.6	
^{224}Th	$\longrightarrow$	^{14}C	+	^{210}Po	33.06	13.6	
	$\longrightarrow$	^{16}O	+	^{208}Pb	46.64	15.0	
^{226}Th	$\longrightarrow$	^{14}C	+	^{212}Po	30.68	18.0	
	$\longrightarrow$	^{18}O	+	^{208}Pb	45.89	18.2	
^{228}Th	$\longrightarrow$	^{14}C	+	^{214}Po	28.34	23.0	
	$\longrightarrow$	^{20}O	+	^{208}Pb	44.87	21.8	20.8
^{230}Th	$\longrightarrow$	^{20}O	+	^{210}Pb	41.96	26.9	
	$\longrightarrow$	^{22}O	+	^{208}Pb	43.34	26.6	
	$\longrightarrow$	^{24}Ne	+	^{206}Hg	57.96	24.8	24.6
^{232}Th	$\longrightarrow$	^{26}Ne	+	^{206}Hg	56.15	29.3	> 27.9
^{230}U	$\longrightarrow$	^{14}C	+	^{216}Rn	28.47	24.7	
	$\longrightarrow$	^{22}Ne	+	^{208}Pb	61.59	20.4	
	$\longrightarrow$	^{24}Ne	+	^{206}Pb	61.55	22.2	
^{232}U	$\longrightarrow$	^{24}Ne	+	^{208}Pb	62.50	20.8	21.1
	$\longrightarrow$	^{28}Mg	+	^{204}Hg	74.54	25.3	
^{234}U	$\longrightarrow$	^{24}Ne	+	^{210}Pb	59.03	25.5	26.0
	$\longrightarrow$	^{28}Mg	+	^{206}Hg	74.35	25.4	25.5
^{236}U	$\longrightarrow$	^{24}Ne	+	^{212}Pb	56.15	29.8	
	$\longrightarrow$	^{26}Ne	+	^{210}Pb	56.94	30.6	
	$\longrightarrow$	^{30}Mg	+	^{206}Hg	72.73	29.1	
^{236}Pu	$\longrightarrow$	^{28}Mg	+	^{208}Pb	79.90	21.3	21.7
^{238}Pu	$\longrightarrow$	^{28}Mg	+	^{210}Pb	76.16	25.6	} 25.7
	$\longrightarrow$	^{30}Mg	+	^{208}Pb	77.26	25.8	
	$\longrightarrow$	^{32}Si	+	^{206}Hg	91.47	25.8	25.3
^{240}Cm	$\longrightarrow$	^{32}Si	+	^{208}Pb	97.83	21.8	
	$\longrightarrow$	^{34}Si	+	^{206}Pb	91.31	27.3	
^{252}Cf	$\longrightarrow$	^{46}Ar	+	^{206}Hg	127.1	29.9	

Tabelle 1: The theoretical values τ_{theor} of (14) are compared to the measured half-lives[10] τ_{exp} for decays from even parent to even daughter nuclei which are always favoured. The energies E_{aA} are given in MeV, the half-lives τ in seconds. The theoretical and experimental values agree generally within a factor of 5; only for $^{228}\text{Th} \rightarrow {}^{20}\text{O} + {}^{208}\text{Pb}$ the theoretical half-life is ten times too large.

$^{A+a}(Z+z)$	$\longrightarrow$	^{a}z	+	^{A}Z	E_{aA}	$\log \tau_{\text{theor}}$	$\log \tau_{\text{exp}}$
^{221}Fr	$\longrightarrow$	^{14}C	+	^{207}Tl	31.40	14.1	
					31.05	14.7	
					30.06	16.7	> 15.8
^{221}Ra	$\longrightarrow$	^{14}C	+	^{207}Pb	32.50	13.0	
					31.93	14.0	
					31.60	14.6	> 14.4
					30.87	16.0	
^{223}Ra	$\longrightarrow$	^{14}C	+	^{209}Pb	31.96	13.8	
					31.18	15.3	15.2
					30.54	16.5	
					30.39	16.8	
^{225}Ac	$\longrightarrow$	^{14}C	+	^{211}Bi	30.59	17.3	17.2
					30.19	18.1	
					29.83	18.9	
^{229}Th	$\longrightarrow$	^{14}C	+	^{215}Po	27.22	25.7	
					26.94	26.3	
					26.92	26.4	
					26.81	26.7	
	$\longrightarrow$	^{20}O	+	^{209}Pb	43.57	24.0	
					42.79	25.4	
					42.15	26.6	
					42.00	26.9	
	$\longrightarrow$	^{24}Ne	+	^{205}Hg	58.02	24.7	
					57.65	25.3	
					57.56	25.4	
					56.17	27.6	
^{231}Pa	$\longrightarrow$	^{24}Ne	+	^{207}Tl	60.61	22.2	
					60.26	22.7	23.4
					59.27	24.1	

Tabelle 2: Cluster radioactive decays from odd parent nuclei to daughter nuclei which are in the ground-state or in selected excited states. The difference $E_{aA}(\text{g.s.}) - E_{aA}(\text{excit.})$ between the tunneling energies is given by the excitation energy E_A^{ex} of the daughter nucleus. The calculated half-lives τ_{theor} apply to *favoured transitions only*. Since the fine structure is usually not resolved, the experimental half-lives τ_{exp} are attached tentatively to favoured transitions in accordance with our calculation. Decays into lower states are then hindered or unfavoured.

$^{A+a}(Z+z)$	$\longrightarrow$	^{a}z	+	^{A}Z	E_{aA}	$\log \tau_{\text{theor}}$	$\log \tau_{\text{exp}}$
^{233}U	$\longrightarrow$	^{24}Ne	+	^{209}Pb	60.69	23.2	
					59.91	24.3	24.8
					59.27	25.2	
					59.12	25.4	
	$\longrightarrow$	^{28}Mg	+	^{205}Hg	74.47	25.3	
					74.10	25.8	
					74.01	25.9	
					72.62	27.7	
^{235}U	$\longrightarrow$	^{24}Ne	+	^{211}Pb	57.55	27.7	27.4
	$\longrightarrow$	^{26}Ne	+	^{209}Pb	58.30	28.4	
					57.52	29.7	
					56.88	30.7	
					56.73	31.0	
	$\longrightarrow$	^{28}Mg	+	^{207}Hg	72.42	27.8	
^{237}Np	$\longrightarrow$	^{30}Mg	+	^{207}Tl	75.25	27.1	
					74.90	27.5	$>$ 27.3
					73.92	28.8	
^{239}Pu	$\longrightarrow$	^{34}Si	+	^{205}Hg	91.11	27.6	
					90.74	28.1	
					90.65	28.2	
					89.26	29.8	
^{241}Am	$\longrightarrow$	^{34}Si	+	^{207}Tl	94.21	25.5	$>$ 25.3
					93.86	25.9	
					92.87	27.0	
^{243}Cm	$\longrightarrow$	^{34}Si	+	^{209}Pb	95.05	25.9	
					94.27	26.7	
					93.62	27.4	
					93.48	27.6	
^{231}Pa	$\longrightarrow$	^{23}F	+	^{208}Pb	52.01	24.7	$>$ 24.6
					49.40	29.1	
					48.81	30.1	
^{233}U	$\longrightarrow$	^{25}Ne	+	^{208}Pb	60.94	23.7	
					58.33	27.6	
					57.74	28.5	
^{235}U	$\longrightarrow$	^{25}Ne	+	^{210}Pb	58.02	27.9	27.4
					57.24	29.2	
					56.94	29.6	

Tabelle 3: Continuation of Table 2. The last entries are decays where the emitted cluster is odd.